SERBIAN JOURNAL OF ELECTRICAL ENGINEERING
Vol. 22, No. 3, October 2025, 437-452

UDC: 517.972.96:004.42MATLAB]:617.583 DOI: https://doi.org/10.2298/SJEE240924006A

Original scientific paper

Terminal Synergetic Control Based Cheetah Optimizer for Knee-Exoskeleton Systems

Huthaifa Al-Khazraji[1], Attariad Khudhair Ahmend[1], Ahmed Ibraheem Abdulkareem[1], Amjad Jaleel Humaidi[1]

Abstract: The knee-exoskeleton is mechanical devices which are designed to help people rehabilitate impaired limb mobility and replace the use of physiotherapists. The scope of this study is rehabilitation assistance for the lower limb (i.e. knee of the leg). Due to the high level of complexity and nonlinearity, various control algorithms have been developed to the knee-exoskeleton system to handle these challenges. This study presents a tracking control design of the angular position for the lower limb exoskeleton knee system based on a terminal synergetic control (TSC) strategy. In addition, the cheetah optimizer (CO) algorithm is introduced and embedded in the design to adjust the design parameters of the controller for further optimization of its performance based on the root mean of square errors (*RMSE*). The superiority of the proposed control method is shown in comparison to the conventional synergetic control (SC) method via computer simulations using MATLAB. The simulations results show that the TSC can improve the response of the system. The numerical value reveals that the *RMSE* is reduced by 14.9%. In addition, the simulation results validate the efficacy of the proposed approach in the presence of external disturbances where the *RMSE* is reduced by 39.1%.

Keywords: Exoskeleton knee system, Lower limb rehabilitation, Nonlinear Control, Terminal synergetic control, Cheetah optimizer.

1 Introduction

The lower human knee joint is important device for wide range of human activities such as walking, running, swimming and cycling. Nevertheless, this joint is subjected to many diseases including musculoskeletal disorders, traumatic

[1]Control and Systems Engineering Department, University of Technology- Iraq, Baghdad, Iraq
60141@uotechnology.edu.iq, https://orcid.org/0000-0002-6290-3382
Attarid.K.Ahmed@uotechnology.edu.iq, https://orcid.org/0000-0001-5461-5949
60162@uotechnology.edu.iq, https://orcid.org/0000-0002-7982-1818
amjad.j.humaidi@uotechnology.edu.iq, https://orcid.org/0000-0002-9071-1329

Colour versions of the one or more of the figures in this paper are available online at https://sjee.ftn.kg.ac.rs

injuries, stroke, and others [1]. As a result of that, there is a remarkable risen in the technology of knee-exoskeleton that has been developed to address these issues. Knee-exoskeleton system is a mechatronic system which is equipped with people suffering from physical weakness in their mobility. Knee-exoskeleton system works as tool for restore human physical capabilities in terms of providing the mechanical support and the strength amplification [2 – 3]. Knee-exoskeleton systems for the lower human knee joint are driven by actuator that provides the suitable torque to accomplish a pre-defined trajectory (i.e. flexion/extension movements) of the lower limbs.

Due to the high level of complexity, nature of human interaction and nonlinearity, various control algorithms have been applied by researchers and engineers to the knee-exoskeleton system to handle these challenges. For example, Rifa et al. [4] introduced a model reference adaptive controller (MRAC) to make the knee-exoskeleton system tracks predefined desired trajectory. The stability was proven based on Lyapunov analysis respect to a bounded human torque. Chevalier et al. [5] investigated the design of fractional-order proportional-integral (FOPI) controller for the movement of the knee-exoskeleton system. A linearized model of the knee-exoskeleton system was used to design the FOIP controller. A model-based tuning approach was used to tune the design variables of the FOPI controller. The simulation results show that FOPI outperforms the integer-order PI controller. Konyak et al. [6] proposed an optimal fuzzy-PID (proportional-integral-derivative) controller is knee-exoskeleton system. The fuzzy controller was used to regulate the gains of the PID controller. The error between the desired angle and actual angle of knee exoskeleton system and the rate of change of tracking error are considered the input variables of the fuzzy controller. The output variables are chosen as the parameters of PID controller. The membership functions of the fuzzy controller are optimized with a well-known optimization algorithm called class topper optimization. The evaluation of the proposed controller is examined under different simulations scenarios. The application of the sliding mode control (SMC) for tracking control of the knee-exoskeleton system was achieved by Waheed and Humaidi [7]. Whale optimization algorithm (WOA) was utilized to obtain the optimal value of the design parameters for further optimization of the SMC performance. The designing of an affine robust feedback control law for position of a knee-exoskeleton system is introduced by [8 – 10]. The stability condition of the proposed controller is guaranteed via Lyapunov approach based on linear matrix inequalities (LMIs). Simulation was used to demonstrate the effectiveness of the proposed control approach. To address the variations in the system parameters and to improve to resistance to external perturbations, Narayan et al. [11] introduced a fast terminal sliding mode integrated with a rapid reaching law (FTSM-RRL) control algorithm. A comparison evaluation has been made between the proposed FTSM-RRL and the FTSM-ERL (fast terminal sliding

mode based exponential reaching law) and the PID controller. The outcomes show that the tracking accuracy and robustness characteristics have been considerably improved by the proposed FTSM-RRL.

These endeavors contribute to the field of controlling the lower limb exoskeleton system. However, a high-performance exoskeleton control system design is still to be developed. This paper proposes a terminal synergetic control (TSC) strategy which is different from the conventional synergetic control (SC) for a knee-exoskeleton system to control the flexion/extension of the knee joint for people with weak knee muscular power and difficulty in walking. Based on previous applications of TSC, TSC has many advantages over other controller approaches such as simple implementation with high efficiency and fast response [12 – 14]. The control law of the TSC is developed based the model of the system and the Lyapunov theorem. The optimal values of the TSC' coefficients are obtained using cheetah optimizer (CO) algorithm. To validate the proposed controller, computer simulations using MATLAB is conducted. First, the performance of the TSC is compared with the SC method, and then, it is compared with published result of the SMC method in the literature based on the root mean of square errors (*RMSE*). The results are presented and evaluated graphically and numerically. Further, proposed controller is evaluated when the system is subjected to an external disturbance.

The main contributions of this paper are summarized as follows:

– A terminal synergetic control strategy is developed for a knee-exoskeleton system to control the flexion/extension of the knee joint for people with weak knee muscular power and difficulty in walking.
– An optimization algorithm based on cheetah optimizer is introduced to tune the design parameters of the proposed controller.
– A comparison study based numerical computer simulations have been conducted between the proposed terminal synergetic control with conventional synergetic control to demonstrating the controller's ability to improve the performance of the system and mitigate the effects of the disturbance effectively using the root mean of square errors index.

The rest of the paper is structured as follows: the mathematical model of the lower limb exoskeleton system is presented in Section 2. In Section 3 and Section 4, the proposed controllers are introduced and the cheetah optimizer is given, respectively. The discussion of the simulation results are given in Section 5. Section 6 summaries the conclusion.

2 Mathematical Model

In this section, the mathematical model of a single-joint knee-exoskeleton system is developed. The objective of the knee-exoskeleton control system is to

produce the torques needed for the knee joint to compensate gravity and the loading forces needed to recreate natural human movements. The mechanical architecture of the exoskeleton comprises two distinct components (superior and inferior) that are configured to operate at the level of the knee, as depicted in Fig. 1.

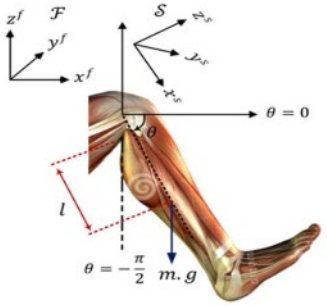

Fig. 1 – *Exoskeleton system* [8].

The superior segment is actuated by a motor and emulates the functionality of the thigh, maintaining a fixed position along the *x*-axis to facilitate the flexion and extension of the knee joint. The inferior segment operates as a shank-foot integrated into the exoskeleton, with its angular motion θ constrained within the limits of 0° to 90°. The exoskeleton system was calibrated to operate within the specified range, as represented in Fig. 1 [4, 9].

Two frames, the local frame S and the global frame $\mathcal{F}$, can be distinguished, from Fig. 1. The frame $(\vec{x}^f, \vec{y}^f, \vec{z}^f)$ defines the global frame, a fixed frame centered on earth. The frame $(\vec{x}^s, \vec{y}^s, \vec{z}^s)$ defines the local frame, also known as the exoskeleton frame. It revolves at the same joint angle, θ, and during the local frame's orientation, the axes of the frames $\vec{y}^f$ and $\vec{y}^s$ coincide. Knee joint movements are seen to have one degree of freedom (DOF) [7].

As a result, the angular velocity of the joint is represented by the time derivative of the knee joint angle $\dot{\theta}$. The equivalent dynamic modeling of the exoskeleton system is established based on Langragian's equation. The latter's mathematical formula can be expressed as follows [15]:

$$\frac{\mathrm{d}}{\mathrm{d}t}\left(\frac{\partial L}{\partial t}\right) - \left(\frac{\partial L}{\partial t}\right) = \tau_{ext}\,. \tag{1}$$

The symbol τ_{ext} represents the external torque exerted on the system. It is made up of three torques as given in (2): the resistive torque (τ_r), which are caused by the solid and viscous frictions in the system, the active torque, which the control torque produced by the DC motor, and the disturbing torque (τ_d)

$$\tau_{ext} = \tau_r + \tau + \tau_d \,. \tag{2}$$

L is the Lagrangian component, which has the following definition:

$$L = E_{ke} - K_{ge} \,. \tag{3}$$

The system's elements' kinetic and gravitational energy are represented by the symbols E_{ke} and K_{ge}, respectively.

$$E_{ke} = \frac{1}{2} J\dot{\theta}, \tag{4}$$

where J denotes the inertia of the system.

$$E_{ge} = mgl\left(1 - \sin\theta\right), \tag{5}$$

where the symbols m, g and l stand for the leg and exoskeleton system mass, gravity-induced acceleration, and the separation between the knee joint and the centre of gravity, respectively. The combined system components' dynamic model can be generated using the Lagrange differential equation of L.

$$J\ddot{\theta} = mgl\cos\theta - \tau_{ext} \,. \tag{6}$$

The system's resistive torque is expressed as follows:

$$\tau_r = -f_{vr}\dot{\theta} - f_{sr}\,\mathrm{sign}\left(\dot{\theta}\right), \tag{7}$$

where $f_{vr}\dot{\theta}$ is the viscous damping torque of the exoskeleton system, $f_{sr}\ \mathrm{sign}\left(\dot{\theta}\right)$ is the solid friction torque of the system and sign(.) is the standard signed function. The system's dynamic modelling can be expressed as follows:

$$J\ddot{\theta} = mgl\cos\theta - f_{vr}\dot{\theta} - f_{sr}\mathrm{sign}\left(\dot{\theta}\right) + \tau + \tau_d \,, \tag{8}$$

$$\tau_g = mgl \,, \tag{9}$$

$$J\ddot{\theta} - \tau_g\ \cos\theta + f_{vr}\dot{\theta} + f_{sr}\mathrm{sign}\left(\dot{\theta}\right) + \tau_d = \tau \,. \tag{10}$$

Equation (10) can be written in the robotic form as follows:

$$M(\theta)\ddot{\theta} + f\left(\theta,\dot{\theta}\right) + G = B(u) \,, \tag{11}$$

where the inertia matrix is denoted by $M(\theta) = J$, the friction force is represented by $f\left(\theta,\dot{\theta}\right) = f_s\mathrm{sign}\left(\dot{\theta}\right) - B_i$, the gravity force at the knee joint is represented by $G(\theta) = \tau_g\cos\theta$, and $Bu = \tau$ defines the torque acting at the knee joint. In terms of acceleration of angular locations, the equation can be expressed as follows based on (11):

$$\ddot{\theta} = M(\theta)^{-1}\left(\tau - f\left(\theta,\dot{\theta}\right) - G(\theta)\right). \tag{12}$$

The following formulation of (12) can be used to express state variables:

$$\dot{x}_1 = \dot{\theta} = x_2 , \tag{13}$$

$$\dot{x}_2 = \ddot{\theta} = \frac{1}{J}\left[\tau - f_{vr}(x_2) - f_{sr}\text{sign}(x_2) + \tau_g \cos(x_1) + \tau_d \right], \tag{14}$$

where the state variable x_2 indicates the knee joint's angular velocity $\dot{\theta}$ and x_1 indicates the knee joint's angular posture θ. For the purpose of controlling design, (14) can be revised as follows:

$$\dot{x}_2 = f(x) + bu , \tag{15}$$

where

$$f(x) = \frac{-f_{vr}(x_2) - f_{sr}\text{sign}(x_2) + \tau_g \cos(x_1) + \tau_d}{J}, \tag{16}$$

$$b = 1/J . \tag{17}$$

3 Controller Design

The advantages of feedback controller approaches to improve system's performance have been demonstrated via a wide range of applications [16 – 18]. Controller design for the knee-exoskeleton system aims to reduce the tracking error between the angular position of the lower human knee joint and pre-defined angular position trajectory. Synergetic control (SC) technique is a simple, robust, nonlinear control algorithm has also been widely used [19 – 20]. One of the main advantages of the applying SC to nonlinear system is that no linearization of the nonlinear system is required. In the following subsections, the procedure to design the both SC and Terminal SC (TSC) for the knee exoskeleton system is given.

3.1 Conventional synergetic control

In the first step, the tracking error e_t is defined as follows:

$$e_t = x_r - x_1 , \tag{18}$$

where x_r is the tracking reference.

In CSC approach, the marco-variable σ is given by:

$$\sigma = \dot{e}_t + \lambda_1 e_t , \tag{19}$$

where λ_1 is a positive scalar tuning coefficient.

Differentiating σ with respect to time obtains:

$$\dot{\sigma} = \ddot{e}_t + \lambda_1 \dot{e}_t . \tag{20}$$

Differentiating e_t with respect to time obtains:

$$\dot{e}_t = \dot{x}_r - \dot{x}_1 = \dot{x}_{1d} - x_2 \,. \tag{21}$$

Differentiating $\dot{e}_t$ with respect to time obtains:

$$\ddot{e}_t = \ddot{x}_r - \dot{x}_2 \,. \tag{22}$$

The following trajectory equation is used to determine the motion of the controlled system:

$$\dot{\sigma} + \lambda_2 \sigma = 0 \,, \tag{23}$$

where λ_1 is a positive scalar tuning coefficient.

Substitute (20), (22) and (15) in (23) gives:

$$\ddot{x}_r - f(x) - bu + \lambda_2 \dot{e}_t + \lambda_2 \sigma = 0 \,. \tag{24}$$

Rearrange (24) to determine u yield:

$$u_{SC} = \frac{1}{b}\left(\ddot{x}_r - f_x + \lambda_1 \dot{e}_t + \lambda_2 \sigma\right). \tag{25}$$

3.2 Terminal synergetic control

The procedure to design TSC is given as follows:

1. The marco-variable σ is defined as

$$\sigma = \lambda_1 e_t^{\,q} + e_t \,, \tag{26}$$

where the power q is a positive less than one.

2. Then, differentiating σ with respect to time obtains,

$$\dot{\sigma} = \lambda_1 q\left(e_t^{1-q}\right)\dot{e}_t + \ddot{e}_t \,. \tag{27}$$

3. Determine the state trajectory of σ as:

$$\dot{\sigma} + \lambda_2 \sigma = 0 \,. \tag{28}$$

4. Substitute $\dot{\sigma}$ gives:

$$\ddot{e}_t + \lambda_1 q\left(e_t^{1-q}\right)\dot{e}_t + \lambda_2 \sigma = 0 \,. \tag{29}$$

5. Substitute $\ddot{e}_t$:

$$\ddot{x}_r - f_x - bu + \lambda_1 q\left(e_t^{1-q}\right)\dot{e}_t + \lambda_2 \sigma = 0 \,. \tag{30}$$

6. Rearrange (30) to determine *u* yield:

$$u_{TSC} = \frac{1}{b}\left(\ddot{x}_r - f_x + \lambda_1 q\left(e_t^{1-q}\right)\dot{e}_t + \lambda_2 \sigma\right). \tag{31}$$

4 Cheetah Optimizer

Optimizing the design parameters of the synergetic control lead to enhance the controller's ability to reject disturbances and maintain performance in the presence of system uncertainties. Due to their ability to solve complex optimization problems, nature-inspired optimization techniques play a prominent role in modern application [21 – 22]. Among these applications is tuning the design parameters of the controllers [23 – 24]. Inspired by the cheetah hunting strategies exhibited in their natural environment, this paper presents the cheetah optimizer algorithm, which is designed to solve large-scale and multi-objective optimization problems.

This algorithm was first introduced in 2022 by Akbari et al. in 2022 [25] and inspired by the hunting strategies used by cheetahs in the wild to ensure their survival. Compared to others metaheuristic algorithms, the cheetah optimizer (CO), performs substantially better and may be used in a variety of optimization situations. To enhance the algorithm's efficiency, the CO uses straightforward methods and hunting strategies. When pursuing prey, cheetahs normally use three main strategies: searching, sitting and waiting, and attacking. The „leave the pray and go back home" tactic is integrated into the hunting process, to enhance performance, convergence, and robustness.

To balance between these strategies, r_1 and r_2 are assumed switching operator. If $r_2 \le r_1$ this mean the cheetah decrease its energy level, therefore sitting and waiting strategy is selected. Otherwise, cheetahs are either in the search mode or attacked mode based on the parameter H and the selected operator r_3, $(0 < r_3 < 3)$. The parameter H is computed as given in (32).

$$H = \mathrm{e}^{(1-t)/T_{\max}} \left(2r_4 - 1\right), \tag{32}$$

where t and $T_{\max}$ are the current and the maximum iteration of the optimization process, r_4 is a random number between 0 and 1. If $H \ge r_3$ attack mode is selected else the search mode is implemented. The mathematical models for hunting tactics are demonstrated in the following subsections and the pseudo-code in Algorithm 1 that illustrate the CO algorithm.

4.1 Search mode

In the exploration phase of this method, the cheetah is in the searching mode, which is searching for food in the surrounding environment. In this stage, the position of a cheetah is determined by using its present location in arrangement J while the location of the prey is determined by the optimal design variable. In this stage, the steps length is randomization.

Algorithm 1. Pseudo-code of CO algorithm

1. **Input**
   - Objective function $\left(F_{xc}\right)$, Population size (N_{pop}),

   Number of decision variables $\left(D_{var}\right)$, Number of iteration $(T_{\max})$
2. **Initialization**
   - Initialize population N_{pop} of cheetahs
   - Evaluate objective function F_{xc} of each cheetah in N_{pop}
   - Assign best position xp
3. **Loop:**
   - **while** $(t < T_{\max})$
     - Determine G_m $(2 < G_m < N_{pop})$
     - **For** each cheetah in G_m
       - ✓ Determine xcl
       - ✓ Update $\hat{r}$, $\breve{r}$ α, β, H
       - ✓ Update r_1, r_2
       - ✓ **If** $r_2 \le r_1$
         - ❖ Update r_3
         - ❖ **If** $H \ge r_3$
           - Update the location cheetah using (38)
         - ❖ **Else**
           - Update the location cheetah using (36)
         - ❖ **End if**
       - ✓ **Else**
           - Update the location cheetah using (37)
       - ✓ **End if**
       - ✓ Update xcl for each G_m
     - **End for**
     - Evaluate F_{xc} and Update $\boldsymbol{xp}$
     - $t = t + 1$
   - **End while**
4. **Print the Optimal Solution**

The step length is determined based on how a cheetah is far away from its neighbor. If the cheetah is currently not the leader, (33) is used to calculate the value for step length.

$$\alpha_{i,j}^{t} = 0.001\frac{t}{T_{\max}}\left(xc_{i,j}^{t} - xc_{q,j}^{t}\right), \tag{33}$$

where $\alpha_{i,j}^{t}$ is the step size of cheetah i in arrangement *j* for iteration *t*, $xc_{i,j}^{t}$ is the current position of cheetah, $xc_{q,j}^{t}$ is a position selected randomly from the population. In case, a cheetah is the current leader then the step length is calculated based on (34).

$$\alpha_{i,j}^{t} = 0.001\frac{t}{T_{\max}}\left(\alpha_{\max}\right), \tag{34}$$

$$\alpha_{\max} = \alpha_{u} - \alpha_{l}, \tag{35}$$

where $\alpha_{\max}$ is the maximum step size, α_{u} and α_{l} are the upper and lower limit respectively. If an opponent appears, the leader will change its direction, to update the new position of the cheetah in each arrangement based on their present position and an arbitrary step size, the next position of cheetah is computed based on (36).

$$xc_{i,j}^{t+1} = xc_{i,j}^{t} + \hat{r}_{i,j}^{-1}\alpha_{i,j}^{t}, \tag{36}$$

where $xc_{i,j}^{t+1}$ is the next locations of cheetah *i* in arrangement *j*. The randomization parameter and the step length of $\alpha_{i,j}^{t}$ for cheetah *i* in arrangement *j* are denoted by $\hat{r}_{i,j}^{-1}$.

4.2 Sit-and-wait mode

In the wild, when a cheetah finds prey, it may choose to wait for the prey to approach before attacking. If the prey doesn't come closer, the cheetah will sit silently and patiently. Essentially, cheetahs will wait for their prey to come close before attacking, as there is a chance that the prey will escape if they are suddenly startled. Since the cheetah is currently not moving, so its next position will be the same as its current one. It is searching for a better solution, which prevents it from converging too soon. The following model is formulated in (37)

$$xc_{i,j}^{t+1} = xc_{i,j}^{t}. \tag{37}$$

4.3 Attack mode

The cheetah will choose to attack when the prey is nearby. The algorithm simulates the exploitation phase as the attack mode. It examines the position, circumstances, and distance between the prey and the cheetah before attacking. Rush and capture are the two phases of the attack method. When the cheetah attacks the prey, it is evident that the prey may try to flee. Cheetahs use their fast speed and flexible physical characteristics to move rapidly and block their prey.

The prey will make every effort to escape, and occasionally hunting attempts will fail. The updated cheetah's position in this mode is defined analytically as given in (38)

$$xc_{i,j}^{t+1} = xc_{B,j}^{t} + \breve{r}_{i,j} \times \beta_{i,j}^{t} . \tag{38}$$

The turning and interaction factors linked to the cheetah *i* in the arrangement *j* are denoted by $\breve{r}_{i,j}$ and $\beta_{i,j}^{t}$ respectively. In the capturing mode, the interaction between the cheetahs or between a cheetah and the leader is reflected in the turning factor $\beta_{i,j}^{t}$. This component is described mathematically as the difference between the position of the *i*-th cheetah and its neighboring.

4.4 Leave prey and go back home

When a hunt fails, the cheetah returns home to recover its energy before starting a new hunt. There are several reasons why a cheetah may give up hunting, such as running out of energy or having a fast target that runs away. In these situations, the cheetah returns home to rest and regain its energy before starting a new hunt. In this mode the cheetah's position was altered to match the prey's current location, meaning that the later position is now equal to the area of the optimal answer. This algorithm makes the exploration phase stronger by keeping the prey position among a small population. The hunting period was reset, and other cheetahs' positions were likewise reset.

5 Computer Simulations and Results

In this section, computer simulations based on MATLAB are performed to evaluate the proposed TSC controller. In this regards, the dynamics of knee-exoskeleton system that are described by (1) – (3) and its physical parameters that are listed in **Table 1** [7] is used in the simulation to represent the dynamics of the system. The performance of the controlled system is simulated for 25 seconds with a zero initial position and velocity. A unit-sin-wave input is used to evaluate control the system.

Table 1

Parameters of knee-exoskeleton system.

Parameter	Value
Inertia (J)	$0.348\,[\mathrm{Kg\,m^2}]$
Solid Friction Coefficient (A)	$0.998\,[\mathrm{Nm}]$
Viscous Friction Coefficient (B)	$0.872\,[\mathrm{Nms/\,rad}]$
Gravity Torque (τ_g)	$3.44\,[\mathrm{Nm}]$

To optimize the performance proposed controllers, the CO is employed to tune the design parameters of the CSC and TSC controllers. To see the impact of the terminal attractor technique, the tuning parameters $(c_1$ and $c_2)$ of the CSC is firstly optimized. Then, the same value obtained for the CSC is used in the TSC. Furthermore, the additional adjustable parameter q is then optimized. The objective function of the CO to tune the performance of the two controllers is based on the root mean of square errors (*RMSE*) as given in (39) [26].

$$RMSE = \sqrt{\frac{1}{n}\sum_{m=1}^{n} e_t^2} \ . \tag{39}$$

The population size (N) of the CO is 20 and the number of Iterations ($T_{\max}$) is 30. **Table 2** lists the design parameters values for the SC and TSC based on the CO algorithm.

Table 2

Optimal setting of controller's design parameters.

Parameters	**Controller**	
	CSC	TSC
c_1	10	10
c_2	50	50
q	-	0.9

The output response of the proposed TSC with the classical SC methods for the angular position of the knee-exoskeleton system is shown in Fig. 2. To determine the effectiveness of the proposed TSC approach, a numerical value of the *RMSE* is reported in **Table 3**.

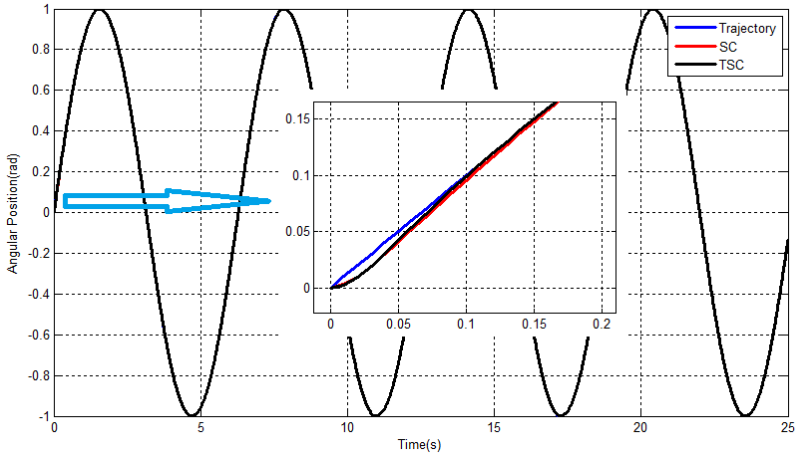

Fig. 2 – *Angular position tracking result.*

Careful observations form the result that is visualized in Fig. 2, it can be say that both SC and TSC remarkably adheres to the desired angular trajectory and deliver the suitable control law to the knee-exoskeleton system. However, the TSC improves the overall performance of the system by reducing the value of the *RMSE* (0.000454) in comparison with the standard SC (0.000534) and the SMC (0.0297). This result means that the *RMSE* with TSC is reduced by 14.9% in compared with SC and 84.7% in compared with SCM. Moreover, as shown in Fig. 3, the chattering phenomenon in the control law of the SMC does not occur in the SC and the TSC.

Table 3
Numerical value of RMSE.

Controller	*RMSE*
TSC	0.000454
SC	0.000534
SMC [7]	0.0297

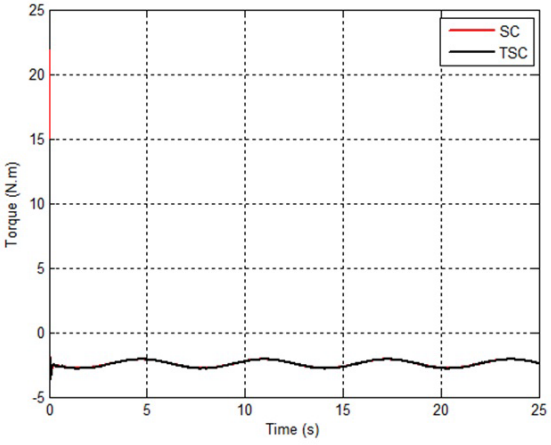

Fig. 3 – *Control input torque.*

To illustrate the resilience of the designed control laws, other numerical simulation is performed for the knee-exoskeleton system under external disturbance. The external disturbance is applied after 10 s of simulation with two second duration time. Fig. 4 shows the tracking performance of the angular position. The angular position for both controller tracks the given reference in the presence of disturbance thus proving the insensitive feature of the SC and TSC. The numerical value of the *RMSE* under disturbance is given in **Table 4**. Based on **Table 4**, it can be revealed that the TSC outperforms the SC by reducing the value of the *RMSE* of TSC (0.0095) in comparison with the standard SC (0.0156).

This result means that the *RMSE* with TSC is reduced by 39.1% in compared with SC.

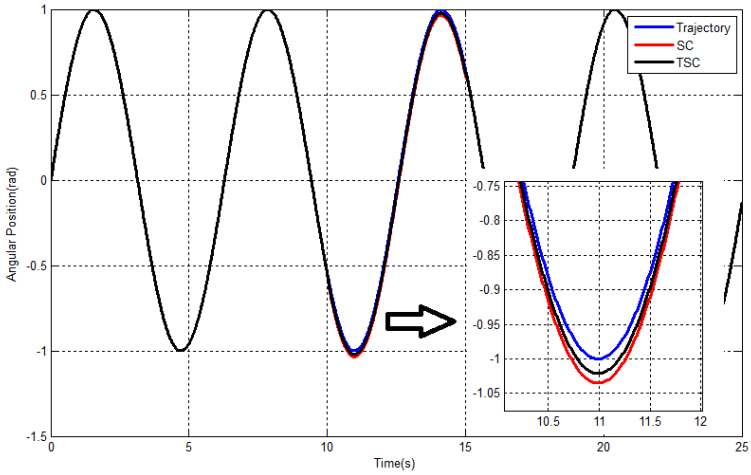

Fig. 4 – *Angular position tracking result with disturbance.*

Table 4
Numerical value of RMSE with disturbance.

Controller	*RMSE*
TSC	0.0095
CSC	0.0156

The aforementioned results of the two scenarios reveal that the additional terminal factor that has been added to the classical SC is capable of effectively improving the responsiveness of controller that is applied to the knee-exoskeleton system. This improvement could be further cross-validated on other systems in the future.

6 Conclusion

In this paper, a terminal synergetic control (TSC) approached has been presented for tracking control of the nonlinear single degree of freedom knee-exoskeleton system. One of the main advantages of the proposed approach is no linearization of the nonlinear system is required and chatter free control law. The cheetah optimizer (CO) algorithm was applied to fine-tune the design parameters for further enhance the controlled system. Computer simulation was conducted to verify the performance of the proposed TSC approach for the knee-exoskeleton system. Numerical results according to *RMSE* as a performance index of the

tracking error indicate that the suggested TSC outperforms the standard SC and the SMC.

7 References

[1] M. S. Fragala, E. L. Cadore, S. Dorgo, M. Izquierdo, W. J. Kraemer, M. D. Peterson, E. D. Ryan: Resistance Training for Older Adults: Position Statement from the National Strength and Conditioning Association, Journal of Strength and Conditioning Research, Vol. 33, No. 8, August 2019, pp. 2019 – 2052.

[2] G. Li, X. Liang, H. Lu, T. Su, Z.- G. Hou: Development and Validation of a Self-Aligning Knee Exoskeleton with Hip Rotation Capability, IEEE Transactions on Neural Systems and Rehabilitation Engineering, Vol. 32, January 2024, pp. 472 – 481.

[3] J.- H. Kim, M. Shim, D. H. Ahn, B. J. Son, S.- Y. Kim, D. Y. Kim, Y. S. Baek, B.- K. Cho: Design of a Knee Exoskeleton Using Foot Pressure and Knee Torque Sensors, International Journal of Advanced Robotic Systems, Vol. 12, No. 8, August 2015, p. 112.

[4] H. Rifaï, S. Mohammed, B. Daachi, Y. Amirat: Adaptive Control of a Human-Driven Knee Joint Orthosis, Proceedings of the IEEE International Conference on Robotics and Automation, Saint Paul, USA, May 2012, pp. 2486 – 2491.

[5] A. Chevalier, C. M. Ionescu, R. De Keyser: Analysis of Robustness to Gain Variation in a Fractional-Order PI Controller for Knee Joint Motion, Proceedings of the International Conference on Fractional Differentiation and Its Applications (ICFDA), Catania, Italy, June 2014, pp. 1 – 6.

[6] N. M. Konyak, D. Acharya, D. Kumar Das: Development of Optimal Fuzzy-PID Controller for an Assistant Human Knee Exoskeleton System, Proceedings of the IEEE Region 10 Conference (TENCON), Chiang Mai, Thailand, October 2023, pp. 777 – 782.

[7] Z. Ali Waheed, A. J. Humaidi: Whale Optimization Algorithm Enhances the Performance of Knee-Exoskeleton System Controlled by SMC, Iraqi Journal of Computers, Communications, Control and Systems Engineering, Vol. 23, No. 2, June 2023, pp. 125 – 135.

[8] S. Jenhani, H. Gritli: LMI-Based Design of an Affine PD Controller for the Robust Stabilization of the Knee Joint of a Lower-Limb Rehabilitation Exoskeleton, Proceedings of the IEEE International Conference on Advanced Systems and Emergent Technologies (IC_ASET), Hammamet, Tunisia, April 2023, pp. 1 – 7.

[9] S. Jenhani, H. Gritli: An LMI-Based Robust State-Feedback Controller Design for the Position Control of a Knee Rehabilitation Exoskeleton Robot: Comparative Analysis, Measurement and Control, Vol. 57, No. 9, October 2024, pp. 1326 – 1346.

[10] S. Jenhani, H. Gritli, J. Narayan: Robust Position Control of a Knee-Joint Rehabilitation Exoskeleton Using a Linear Matrix Inequalities-Based Design Approach, Applied Sciences, Vol. 15, No. 1, January 2025, p. 404.

[11] J. Narayan, H. Gritli, S. K. Dwivedy: Fast Terminal Sliding Mode Control with Rapid Reaching Law for a Pediatric Gait Exoskeleton System, International Journal of Intelligent Robotics and Applications, Vol. 8, No. 1, March 2024, pp. 76 – 95.

[12] H. Benbouhenni, N. Bizon: Terminal Synergetic Control for Direct Active and Reactive Powers in Asynchronous Generator-Based Dual-Rotor Wind Power Systems, Electronics, Vol. 10, No. 16, August 2021, p. 1880.

[13] A. Boonyaprapasorn, S. Simatrang, S. Kuntanapreeda, T. Sethaput: Application of the Terminal Synergetic Control for Biological Control of Sugarcane Borer, IEEE Access, Vol. 12, April 2024, pp. 49562 – 49577.

[14] M. Nawfal, A. A. Yahya, R. A. Mahmod, H. Al-Khazraji: Integration of Sparrow Search Optimization with Terminal Synergetic Control for Permanent Magnet Linear Synchronous Motors, Journal of Robotics and Control, Vol. 6, No. 2, April 2025, pp. 1033 – 1040.

[15] R. A. Kadhim, M. Q. Kadhim, H. Al-Khazraji, A. J. Humaidi: Bee Algorithm Based Control Design for Two-Links Robot Arm Systems, IIUM Engineering Journal, Vol. 25, No. 2, July 2024, pp. 367 – 380.

[16] F. R. Yaseen, M. Q. Kadhim, H. Al-Khazraji, A. J. Humaidi: Decentralized Control Design for Heating System in Multi-Zone Buildings Based on Whale Optimization Algorithm, Journal Européen des Systèmes Automatisés, Vol. 57, No. 4, August 2024, pp. 981 – 989.

[17] F. R. Al-Ani, O. F. Lutfy, H. Al-Khazraji: Optimal Backstepping and Feedback Linearization Controllers Design for Tracking Control of Magnetic Levitation System: A Comparative Study, Journal of Robotics and Control, Vol. 5, No. 6, October 2024, pp. 1888 – 1896.

[18] Z. N. Mahmood, H. Al-Khazraji, S. M. Mahdi: Adaptive Control and Enhanced Algorithm for Efficient Drilling in Composite Materials, Journal Européen des Systèmes Automatisés, Vol. 56, No. 3, June 2023, pp. 507 – 512.

[19] H. Al-Khazraji, K. Al-Badri, R. Al-Majeez, A. J. Humaidi: Synergetic Control Design Based Sparrow Search Optimization for Tracking Control of Driven-Pendulum System, Journal of Robotics and Control, Vol. 5, No. 5, August 2024, pp. 1549 – 1556.

[20] F. R. Al-Ani, O. F. Lutfy, H. Al-Khazraji: Optimal Synergetic and Feedback Linearization Controllers Design for Magnetic Levitation Systems: A Comparative Study, Journal of Robotics and Control, Vol. 6, No. 1, November 2024, pp. 22 – 30.

[21] H. Al-Khazraji, S. Khlil, Z. Alabacy: Industrial Picking and Packing Problem: Logistic Management for Products Expedition, Journal of Mechanical Engineering Research and Developments, Vol. 43, No. 2, 2020, pp. 74 – 80.

[22] H. Al-Khazraji: Comparative Study of Whale Optimization Algorithm and Flower Pollination Algorithm to Solve Workers Assignment Problem, International Journal of Production Management and Engineering, Vol. 10, No. 1, January 2022, pp. 91 – 98.

[23] A. K. Ahmed, H. Al-Khazraji, S. M. Raafat: Optimized PI-PD Control for Varying Time Delay Systems Based on Modified Smith Predictor, International Journal of Intelligent Engineering and Systems, Vol. 17, No. 1, February 2024, pp. 331 – 342.

[24] M. K. Hamzah, L. T. Rasheed: Design of Optimal Sliding Mode Controllers for Electrical Servo Drive System Under Disturbance, AIP Conference Proceedings, Vol. 2415, No. 1, December 2022, p. 030005.

[25] H. Al-Khazraji, W. Guo, A. J. Humaidi: Improved Cuckoo Search Optimization for Production Inventory Control Systems, Serbian Journal of Electrical Engineering, Vol. 21, No. 2, June 2024, pp. 187 – 200.

[26] M. A. Akbari, M. Zare, R. Azizipanah-Abarghooee, S. Mirjalili, M. Deriche: The Cheetah Optimizer: A Nature-Inspired Metaheuristic Algorithm for Large-Scale Optimization Problems, Scientific Reports, Vol. 12, 2022, p. 10953.

[27] M. A. AL-Ali, O. F. Lutfy, H. Al-Khazraj: Comparative Study of Various Controllers Improved by Swarm Optimization for Nonlinear Active Suspension Systems with Actuator Saturation, International Journal of Intelligent Engineering and Systems, Vol. 17, No. 4, August 2024, pp. 870 – 881.